RESEARCH PAPER

Cancer Biology & Therapy 15:5, 643–650; May 2014; © 2014 Landes Bioscience

Mice lacking G0S2 are lean and cold-tolerant

Tian Ma[1], Alexandra GN Lopez-Aguiar[1], Aihua Li[2], Yun Lu[1], David Sekula[1], Eugene E Nattie[2], Sarah Freemantle[1], and Ethan Dmitrovsky[1,3,4]

[1]Department of Pharmacology and Toxicology; Geisel School of Medicine at Dartmouth; Hanover, NH USA; [2]Department of Physiology and Neurobiology; Geisel School of Medicine at Dartmouth; Hanover, NH USA; [3]Department of Medicine; Geisel School of Medicine at Dartmouth; Hanover, NH USA; [4]Norris Cotton Cancer Center; Dartmouth-Hitchcock Medical Center; Lebanon, NH USA

Keywords: G0S2, tumor suppressor, knockout mice, metabolism, body weight, cold tolerance, lactation

Abbreviations: APL, acute promyelocytic leukemia; ATGL, adipose triglyceride lipase; BAT, brown adipose tissue; CIDEA, cell death-inducing DNA fragmentation factor-α-like effector A; DAG, diglyceride; FA, fatty acid; FFA, free fatty acid; G0S2, G_0/G_1 switch gene 2; HFD, high fat diet; MAG, monoglyceride; PGC1-α, PPARγ coactivator 1α; PYPH, phytanoyl-CoA dioxygenase; RQ, respiratory quotient; TAG, triglyceride; UCP-1, uncoupling protein-1; WAT, white adipose tissue; WT, wild-type

G_0/G_1 switch gene 2 (G0S2) is a protein that was first identified in a search for lymphocyte G_0/G_1 switch genes. A direct role for G0S2 in cell cycle regulation has proven elusive. Yet, there is prior evidence for G0S2 functioning in tumor suppression, immune regulation and lipolysis. To explore definitively G0S2 functions, mice lacking G0S2 were generated and characterized. $G0S2^{-/-}$ mice were born at a Mendelian ratio and were phenotypically normal, with the exception of a possible lactation defect. $G0S2^{-/-}$ female mice carried viable pups to term, but could not typically sustain them beyond 48 h. G0S2 is shown here to be most highly expressed in adipose tissue. It is also expressed in liver, skeletal muscle, lung, ventricles of the heart, and components of the kidney. G0S2 loss significantly decreased relative body weight gain as compared with wild-type (WT) ($G0S2^{+/+}$) mice, with a significant decrease in gonadal fat pad weight and a significant increase in serum glycerol levels. This decreased relative body weight gain is not associated with a significant decrease in food intake or increase in activity of $G0S2^{-/-}$ mice. In fact, $G0S2^{-/-}$ mice were significantly less active at night than $G0S2^{+/+}$ mice. When fed with a high fat diet (45% fat diet), G0S2 loss did not prevent diet-induced obesity in mice. Intriguingly, G0S2 loss improved acute cold tolerance, augmenting expression of genes involved in thermogenesis. In summary, in vivo roles for G0S2 were found in lactation, energy balance, and thermogenesis. This study provides a basis for tumor suppressive effects of G0S2 by regulating lipolysis.

Introduction

G_0/G_1 switch gene 2 (G0S2) was first discovered in a search for lymphocyte G_0/G_1 switch genes that regulate cell cycle progression in cultured human mononuclear cells following lymphocyte mitogen lectin treatment.[1] However, a specific role for G0S2 in cell cycle progression from the G_0 phase of the cell cycle has not yet been established. G0S2 is abundantly expressed in adipose tissue, and is also expressed in other tissues such as liver and hematopoietic cells.[2-5] When acute promyelocytic leukemia (APL) cells were treated with all-*trans* retinoic acid to induce differentiation and reduce tumorigenicity, G0S2 levels were markedly induced.[6] Transcriptional regulation of G0S2 is cell context-dependent. For instance, G0S2 is a PPAR target gene in adipocyte and hepatocytes, but its level is not inducible by PPAR agonists in APL cells (unpublished data and Zandbergen et al.).[4]

Several studies have found downregulated expression of G0S2 in a range of cancers, including clinical lung adenocarcinoma, squamous cell carcinomas, and in cancer cell lines of lung, breast, and colon origins.[7] Moreover, knockdown of G0S2 increased E1A and ras-induced transformation of murine embryonic fibroblasts, indicating a potential role of G0S2 in carcinogenesis.[7] Hypermethylation of the G0S2 promoter was found in primary head and neck squamous cell carcinoma, primary squamous lung cancer, and also in squamous lung cancer cell lines.[8-10] This epigenetic silencing of G0S2 in diverse types of cancer strengthens the case for G0S2 acting as a tumor suppressor. In vitro modification of G0S2 levels has shown little impact on cell growth, apoptosis or differentiation (unpublished data and Kusakabe et al.).[8] A few cell lines have been described that are sensitive to G0S2 overexpression but the functional relevance of these high levels of G0S2 is unclear.[7]

Consistent with its abundant expression in adipose tissue, G0S2 was recently found to be involved in lipolysis in vitro and ex vivo by inhibiting the activity of adipose triglyceride lipase (ATGL).[2] Lipolysis is triggered when energy needs exceed available nutrient levels and when there is an increased requirement for lipid membrane substrates.[11] During lipolysis, triglycerides (TAG), which are stored in cellular lipid droplets, are first hydrolyzed to diglycerides (DAG), then to monoglycerides (MAG), and finally to glycerol. In each step, one fatty acid (FA) is released as an energy substrate. The first and rate-limiting step of lipolysis

*Correspondence to: Ethan Dmitrovsky; Email: ethan.dmitrovsky@dartmouth.edu
Submitted: 02/13/2014; Accepted: 02/15/2014; Published Online: 02/20/2014
http://dx.doi.org/10.4161/cbt.28251

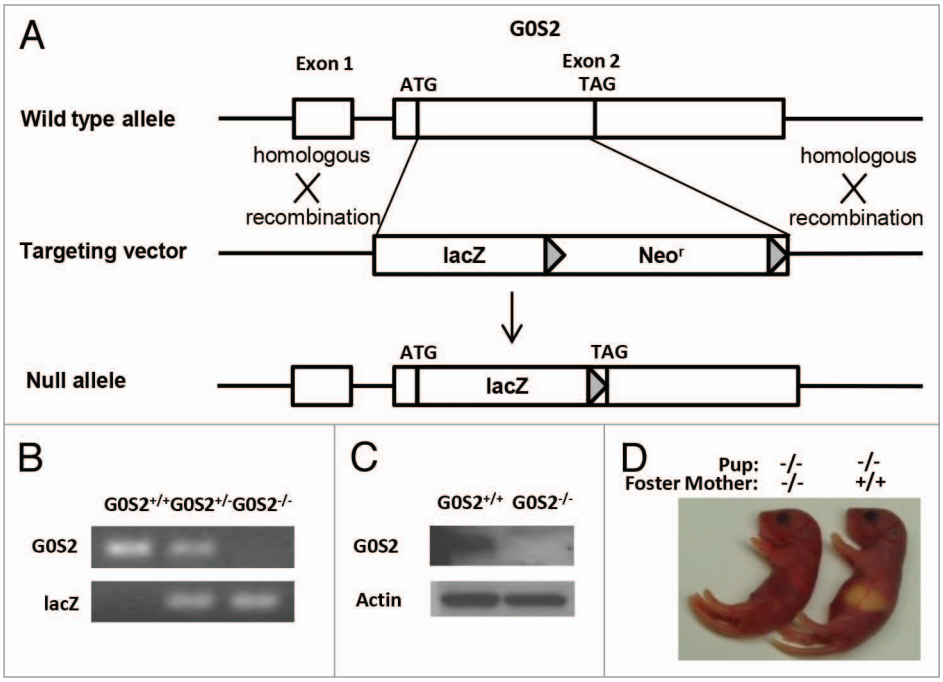

Figure 1. Generation of G0S2$^{-/-}$ mice. (**A**) Targeting strategy of G0S2$^{-/-}$ mice. Homologous recombination of the targeting vector with the wild type (WT) allele resulted in the replacement of the G0S2 coding region with a lacZ and loxP-flanked neomycin resistance gene cassette. (**B**) Genotyping of WT (G0S2$^{+/+}$), heterozygote (G0S2$^{+/-}$), and homozygote (G0S2$^{-/-}$) mice with primers for G0S2 and lacZ. (**C**) Immunoblot analysis of G0S2 protein expression with proteins from gonadal fat of G0S2$^{+/+}$ and G0S2$^{-/-}$ mice. Actin served as loading control. (**D**) Evidence for lactation defects in G0S2$^{-/-}$ mice. A representative G0S2$^{-/-}$ pup fed with a G0S2$^{-/-}$ mother did not have a visible milk spot as seen in a pup nursed by a G0S2$^{+/+}$ mother.

is primarily mediated by ATGL.[12] G0S2 was recently found to be a negative regulator of ATGL, inhibiting its activity by binding to the patatin-like lipolytic domain of the enzyme.[2] And this inhibition is independent of CGI-58 activation, which is another regulator of ATGL activity.[2] G0S2 knockdown increased lipolysis, while G0S2 overexpression decreased lipolysis in vitro in murine and human adipocyte cell lines as well as ex vivo in murine fat pads.[2,3]

To explore directly the consequences of G0S2 loss in an animal model, knockout mice were generated and characterized. G0S2 null mice were born at a normal Mendelian ratio and are phenotypically normal, with the exception of a potential lactation defect. G0S2 null mice have decreased relative body weight with decreased fat pad weight. Notably, G0S2 loss also improved acute cold tolerance. This was associated with enhanced expression of genes that regulate thermogenesis and FA oxidation. The findings presented here define an in vivo role for G0S2 in energy balance.

Results

Generation of G0S2$^{-/-}$ mice

To investigate G0S2 function in vivo, mice lacking G0S2 were generated. In brief, the G0S2 coding region was replaced by a lacZ and loxP-flanked neomycin resistance gene cassette (**Fig. 1A**). The lacZ gene was fused in-frame with a G0S2 start codon. Embryonic stem cells that underwent homologous recombination into the G0S2 gene were selected and injected into blastocysts to generate G0S2$^{+/-}$ mice. Genotypes of G0S2$^{+/+}$, heterozygous (G0S2$^{+/-}$), and null (G0S2$^{-/-}$) mice were confirmed by DNA analysis of G0S2 and lacZ (**Fig. 1B**). To establish the loss of G0S2 at the protein level, white adipose tissues, which is known to have substantial G0S2 expression,[2] were independently harvested from G0S2$^{+/+}$ and G0S2$^{-/-}$ mice. Immunoblot assays confirmed the absence of G0S2 protein in murine G0S2$^{-/-}$ mouse tissues (**Fig. 1C**).

G0S2 mice were born at a normal Mendelian ratio, and they had a normal phenotype, with the exception that while G0S2$^{-/-}$ mothers can carry pups to term, the pups typically do not survive beyond 48 h. Pups from G0S2 null mothers had no visible milk spot as seen in pups from G0S2$^{+/+}$ or G0S2$^{+/-}$ mothers (**Fig. 1D**). Fostering these pups with murine G0S2$^{+/+}$ mothers allowed them to survive at normal ratios. G0S2 is involved in lipid metabolism, and lipids are energy sources in milk.[13] It is then not surprising that G0S2$^{-/-}$ mice had a lactation defect.

G0S2 tissue distribution

The lacZ gene is fused in-frame with the G0S2 start codon, and therefore is regulated by the G0S2 promoter. Three-month-old male G0S2$^{-/-}$, G0S2$^{+/-}$, and G0S2$^{+/+}$ mice were used and diverse organs were subjected to lacZ staining to determine the distribution of G0S2 expression. As indicated by lacZ staining in G0S2$^{-/-}$ mice, G0S2 was abundantly expressed in white adipose tissue (WAT) and liver (**Fig. 2**). It was also expressed in skeletal muscle, lung, heart ventricles, but not in the atrium of the heart or components of the kidney, (**Fig. 2**). Brown adipose tissue (BAT) also had abundant expression of G0S2 (data not shown).

Loss of G0S2 decreased relative body weight gain and reduced fat pad weight

Since G0S2 has a negative regulatory role on lipolysis in vitro and ex vivo, the effects of G0S2 on body weight and body fat were investigated in these mice. Male G0S2$^{+/+}$ and G0S2$^{-/-}$ mice at 8 wk of age were fed with either control diet (10% fat diet) or high fat diet (HFD, 45% fat diet) for 14 wk. Before being fed with these special diets, G0S2$^{+/+}$ and G0S2$^{-/-}$ mice had similar body weights at 8 wk of age (data not shown). Body weights of mice were normalized to individual initial body weights of mice at 8 wk of age and evaluated during the course of the experiment, and this normalized value was termed as relative body weight. G0S2$^{-/-}$ mice fed with a control diet (10% fat diet) had

a significant decrease in relative body weight as compared with G0S2$^{+/+}$ mice after 2 wk fed on the diet (**Fig. 3A**, upper panel), while having similar food intake as compared with G0S2$^{+/+}$ mice (**Fig. 3A** lower panel). There was one time point at the age of week 19 that showed a trend of decreased relative body weight, and this was related to an increased food intake of G0S2$^{-/-}$ mice during that week (**Fig. 3A**). Although there was no difference in the individual organ weights of heart, lung, pancreas, spleen, kidney, testis, and brain, there was a trend of decreased liver weight in G0S2$^{-/-}$ vs. G0S2$^{+/+}$ mice (**Fig. 3C**, left panel). Additionally, the gonadal fat pad weighed significantly less than in controls, and the inguinal and renal fat pads had a trend of decreased weight in G0S2$^{-/-}$ mice (**Fig. 3C**, right panel). Consistent with a role for G0S2 in lipolysis inhibition, serum glycerol levels were significantly elevated in G0S2$^{-/-}$ mice, and there was a trend of increased serum free fatty acid (FFA) levels in G0S2$^{-/-}$ mice (**Fig. 4**).

G0S2$^{-/-}$ mice had a trend toward increased O_2 consumption in the dark

Because G0S2$^{-/-}$ mice had decreased relative body weight, but similar food intake as compared with G0S2$^{+/+}$ mice, it was possible that they had an increased metabolism. O_2 consumption was evaluated as an indicator of metabolism. Interestingly, there was a trend toward increased levels of O_2 consumption in G0S2$^{-/-}$ mice exposed to the dark (**Fig. 5A**). These mice had a significantly lower percentage of active time at some time points during the dark cycle (**Fig. 5C**). Because of the recently shown role of G0S2 in lipolysis, the effect of G0S2 loss on energy substrate usages (e.g., carbohydrates vs. lipids) was examined by evaluating the respiratory quotient (RQ). Mice fed with HFD (45% fat diet) showed a decreased RQ as compared with those fed with a control diet (10% fat diet) (**Fig. 5B**), confirming more lipid usage as an energy substrate. G0S2$^{-/-}$ mice did not show a difference in RQ as compared with G0S2$^{+/+}$ mice, both in the control diet (10% fat diet) and HFD diet group (45% fat diet). This establishes that G0S2$^{-/-}$ mice have similar energy substrate usage as G0S2$^{+/+}$ mice.

G0S2$^{-/-}$ mice exhibit enhanced acute cold tolerance

The effect of G0S2 loss on another metabolism parameter, thermoregulation, was examined. G0S2$^{+/+}$ and G0S2$^{-/-}$ mice were exposed to 4 °C ambient temperature for 3 h, and their body temperatures were recorded immediately before and during the cold exposure. G0S2$^{-/-}$ mice fed with a 10% diet were able to maintain their body temperature for longer times than for G0S2$^{+/+}$ mice (**Fig. 6A**), despite having reduced fat pad weight (**Fig. 3C**, right panel). Beyond physical insulation (body fat and fur), body temperature upon acute cold exposure is maintained by both shivering (muscle-mediated) and non-shivering (primarily BAT-mediated) thermogenesis.[14,15] No obvious differences in mouse behavior or the muscle shivering intensity were observed in these mice (data not shown). To assess differences in non-shivering thermogenesis, key gene products that are involved in thermogenesis and FA oxidation were examined in BAT following 3 h cold treatment of mice. We found out that uncoupling protein-1 (UCP-1), PPARγ coactivator 1α (PGC1-α), phytanoyl-CoA dioxygenase (PHYH), and cell death-inducing DNA fragmentation factor-α-like effector A (CIDEA), were all

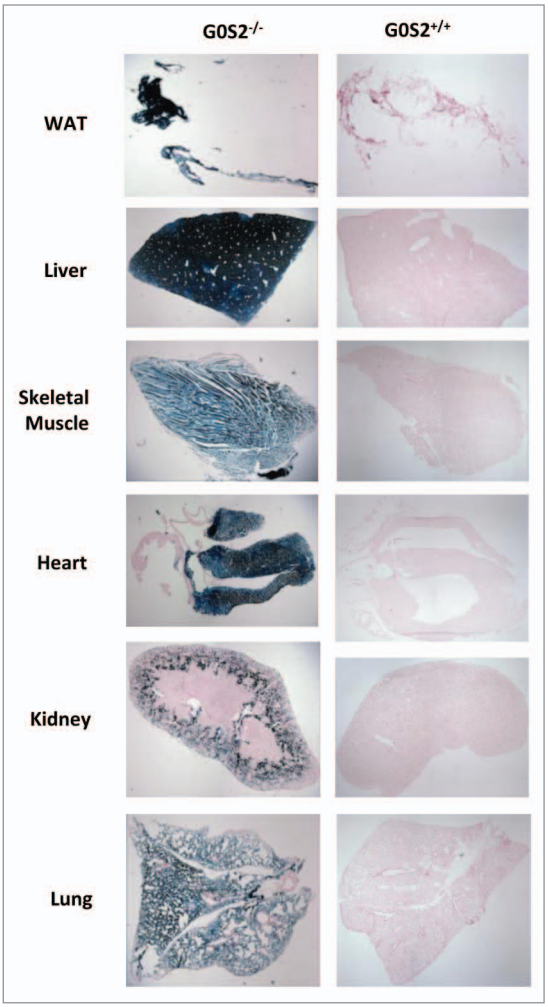

Figure 2. G0S2 tissue distribution in various organs. Organs from 3 mo old male G0S2$^{-/-}$ and G0S2$^{+/+}$ mice were independently harvested and lacZ stainings were performed in white adipose tissue (WAT), liver, skeletal muscle, heart, kidney, and lung tissues.

significantly elevated in G0S2$^{-/-}$ mice (**Fig. 6C**). PPARα also had a trend toward increased expression in G0S2$^{-/-}$ mice (P = 0.07) (**Fig. 6C**). These elevated thermoregulatory species in BAT indicate that G0S2$^{-/-}$ mice have enhanced non-shivering thermogenesis. G0S2$^{-/-}$ mice fed with a 45% fat diet also had improved cold tolerance as compared with G0S2$^{+/+}$ mice (**Fig. 6B**).

Discussion

G0S2 is a gene product that is implicated in diverse cellular activities, and is frequently deregulated in cancer.[7-10,16-18] However, its functions are still not well understood. To explore G0S2 function in vivo, G0S2$^{-/-}$ mice were generated and characterized (**Fig. 1**). G0S2 was abundantly expressed in the adipose tissue and liver, and was also expressed in the skeletal muscle, lung, the heart ventricles, but not the atrium of the heart and the cortical region of the kidney (**Fig. 2**). Although G0S2$^{-/-}$ mice had a similar food intake as compared with G0S2$^{+/+}$ mice, they had

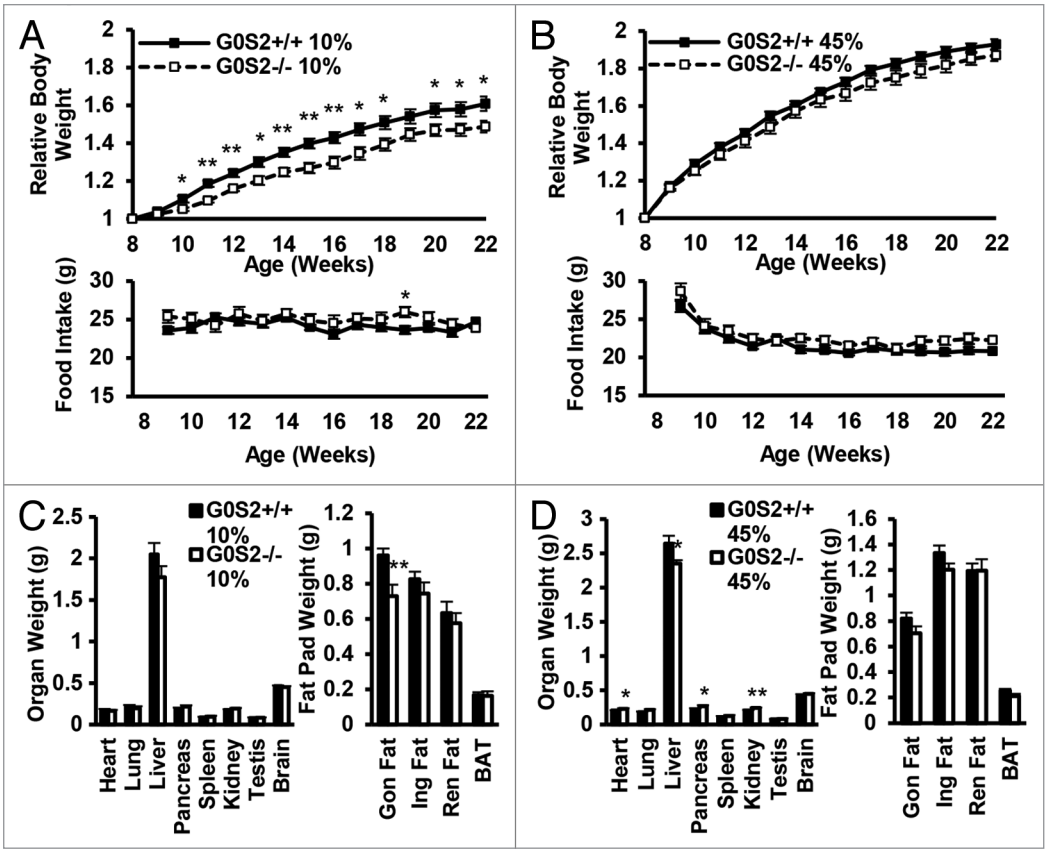

Figure 3. G0S2$^{-/-}$ mice showed decreased relative body weight and decreased fat pad weight. (**A and B**) Relative body weight as compared with initial body weight (8 wk of age) of male G0S2$^{+/+}$ and G0S2$^{-/-}$ mice during 14 wk fed on a 10% fat diet (**A**, upper panel) or a 45% fat diet (**B**, upper panel). Food intake of G0S2$^{+/+}$ and G0S2$^{-/-}$ mice during 14 wk on a 10% fat diet (**A**, lower panel) and 45% fat diet (**B**, lower panel) (n = 12). (**C and D**) Organ weight (left panel) and fat pad weight (right panel) of male mice fed a 10% fat diet (**C**) and 45% fat diet (**D**) (n = 8–9). Gon Fat, gonadal fat pad; Ing Fat, inguinal fat pad; Ren fat, renal fat pad; BAT, interscapular brown adipose tissue. The symbols * and ** depict statistical significance as $P < 0.05$ and $P < 0.01$, respectively.

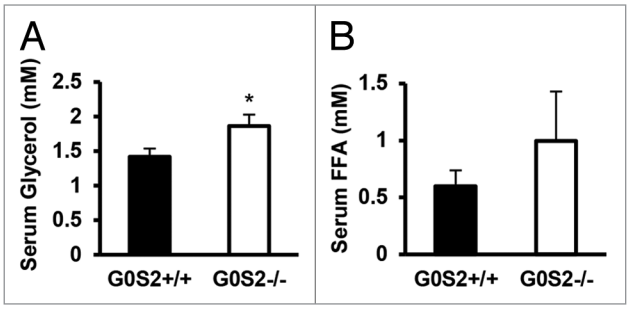

Figure 4. Serum glycerol and free fatty acid levels in G0S2$^{+/+}$ and G0S2$^{-/-}$ mice. Serum from 5 mo old male G0S2$^{+/+}$ and G0S2$^{-/-}$ mice fed with 10% fat diet were analyzed for (**A**) glycerol and (**B**) free fatty acid (n = 11–12). Data are presented as mean ± SE. The symbol * depicts statistical significance as $P < 0.05$.

decreased relative body weight when fed with a 10% fat diet, and had decreased gonadal fat pad weight (**Fig. 3**). Increased serum glycerol and possibly FFA levels was also consistent with increased lipolysis in the adipose tissue (**Fig. 4**). Although G0S2$^{-/-}$ mice had a reduced percentage of active time in the dark, their O_2 consumption was similar and sometimes higher as compared with G0S2$^{+/+}$ mice (**Fig. 5**). And even though G0S2$^{-/-}$ mice had reduced fat pad weight, they had improved cold tolerance, likely due to enhanced activation of thermogenesis and FA oxidation upon cold exposure in BAT (**Fig. 6**).

The distribution expression profile for G0S2 in diverse organs at the cellular level in adult mice was previously unknown. The abundant expression levels of G0S2 in adipose tissue and liver (**Fig. 2**) were consistent with previous findings,[2-4] implying an important functional role for G0S2 in these tissues. Interestingly, G0S2 was only expressed in the ventricle but not the atrium of the heart, although both regions are composed of cardiac muscle (**Fig. 2**). This implied that G0S2 was likely involved in activities that are specific for ventricular function in the heart, and further studies are needed to elucidate the precise physiological relevance of this differential expression.

Defective lipid metabolism may play an important role in the lactation defect as seen in G0S2$^{-/-}$ mothers. Mice lacking adipophilin, another protein involved in TAG metabolism, also show lactation defects and inability to sustain pups.[19] However, the lactation defect upon G0S2 loss may be ATGL independent, as there is to our knowledge no prior evidence for altered lactation in ATGL deregulated mice. Studies are ongoing to investigate mechanisms of potential lactation defects in G0S2$^{-/-}$ mice.

In contrast to the in vitro and ex vivo studies that showed substantial inhibition of adipose lipolysis upon G0S2 overexpression,[2] G0S2 loss exerted a moderate decrease in fat pad weight decrease in vivo. And it did not prevent diet-induced obesity when male G0S2$^{-/-}$ mice were fed with 45% HFD (**Fig. 3B**). This was surprising given the expected role of G0S2 as an inhibitor of adipose lipolysis, and was in contrast to marked phenotypes observed in mice with deregulated ATGL expression. ATGL-deficient mice had a notable decrease in adipose lipase activity and a substantial increase in adipocyte size, body fat content, and body weight.[12] Mice with adipose-specific ATGL overexpression also had a decrease in adipocyte size, body fat content, and body

weight on HFD.[20] G0S2 regulates ATGL activity via a protein–protein interaction, and not all ATGL in adipocytes may be bound to G0S2,[2] therefore G0S2 may only regulate a fraction of total ATGL activity in adipocytes. This may explain the moderate effect on lipolysis in vivo. In addition, there might be a compensatory mechanism in adipocytes following G0S2 loss, such as downregulation of CGI-58, which is the positive regulator of ATGL, as well as downregulation of HSL, TGH, and TGH-2, which also have TAG lipase activities.[21-23]

Interestingly, G0S2$^{-/-}$ mice had a decreased percentage of active time during the night period (**Fig. 4**). It is possible that G0S2 loss led to decline in motor activity and/or a decrease in the time mice were awake in the dark. This may also be independent of ATGL function, as adipose-specific ATGL transgenic mice did not have a difference in locomotor activity.[20] Despite the lower percentage of active time, G0S2$^{-/-}$ mice had a trend toward increased O_2 consumption as compared with G0S2$^{+/+}$ mice maintained in the dark. Therefore, physiological activities which are not associated with locomotor activity, such as increased body temperature in the dark, may play a key role in this increased trend of energy expenditure. The acute cold tolerance test measures shivering and non-shivering mechanisms to maintain body temperature. The observation of increased expression of genes involved in thermogenesis and oxidation in BAT of G0S2$^{-/-}$ mice is consistent with increased non-shivering thermogenesis (**Fig. 6**). BAT has been long recognized as the primary tissue responsible for non-shivering thermogenesis upon cold exposure. Recently, studies have shown that other tissues may also be involved in non-shivering thermogenesis including WAT, where β3-adrenergic receptor activation increases metabolic rate and body temperature, which seems to be independent of UCP-1 expression.[24] In addition, overexpression of lipoprotein lipase in skeletal muscle enhanced cold tolerance by shifting the muscle fiber type toward the more oxidative type IIa and increasing fat oxidization capability.[25] Muscle activity was also thought to be enhanced with increased mitochondria content and increased total ATP capacity in UCP-1 knockout mice.[26] Therefore, although we did not observe changes in shivering of G0S2$^{-/-}$ mice, it is possible that G0S2$^{-/-}$ mice have enhanced heat generation in their muscles as compared with G0S2$^{+/+}$ mice. In addition, non-shivering thermogenesis in tissues other than BAT, such as WAT and skeletal muscles, may also be involved in the enhanced acute cold tolerance as seen in G0S2$^{-/-}$ mice.

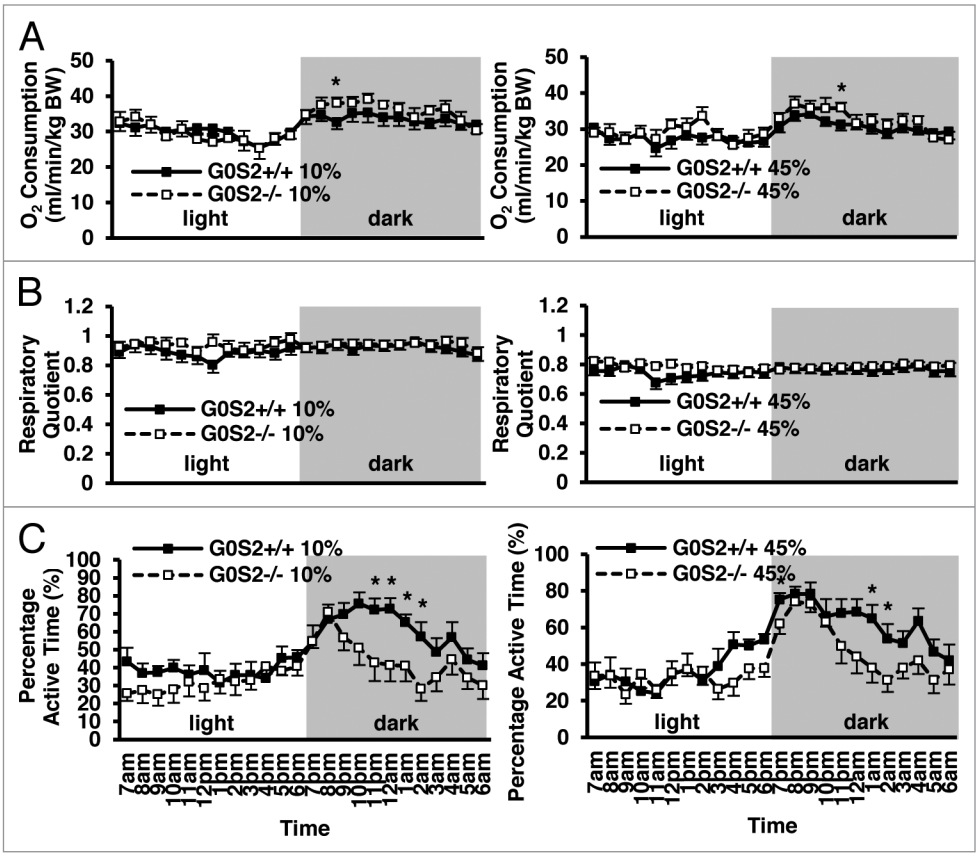

Figure 5. O_2 consumption, respiratory quotient and percentage active time of G0S2$^{-/-}$ mice vs. G0S2$^{+/+}$ mice. (**A–C**) Time course of (**A**) O_2 consumption, (**B**) respiratory quotient, and (**C**) percentage active time of G0S2$^{+/+}$ vs. G0S2$^{-/-}$ male mice fed a 10% fat diet (left panel) or a 45% fat diet (right panel) during 24 h with access to food and water ad libitum (n = 12). Data are presented as mean ± SE. The symbol * depicts statistical significance as $P < 0.05$.

Whether the effect of G0S2 in vivo is through G0S2 itself, or through its interacting proteins, is still under investigation. The in vitro effect of G0S2 on adipocyte lipolysis was through its interaction with ATGL.[2] G0S2 has also been shown to interact with the anti-apoptotic protein Bcl-2 when overexpressed in non-squamous lung cancer cells and colon cancer cells, resulting in apoptosis.[7] In hematopoietic progenitor cells as well as in human APL cell line, G0S2 was also found to bind to nucleolin, which is known to be involved in rRNA synthesis, chromatin remodeling and cell proliferation.[5,27,28] This binding results in the cytoplasmic retention of nucleolin and decreased proliferation of these cells.[5,27] Given accumulating evidence for G0S2 as a potential tumor suppressor, we are planning to examine the in vivo effect of G0S2 loss on tumorigenesis.

In summary, G0S2$^{-/-}$ mice are born at a normal Mendelian ratio and are phenotypically normal except for an apparent lactation defect in G0S2$^{-/-}$ mothers. G0S2$^{-/-}$ mice have decreased relative body weight, decreased fat pad weight, but were more cold tolerant than G0S2$^{+/+}$ mice. Studies are underway to explore how G0S2 loss in mice upregulates expression of thermogenic genes in BAT, and how G0S2 loss leads to lactation defects. This

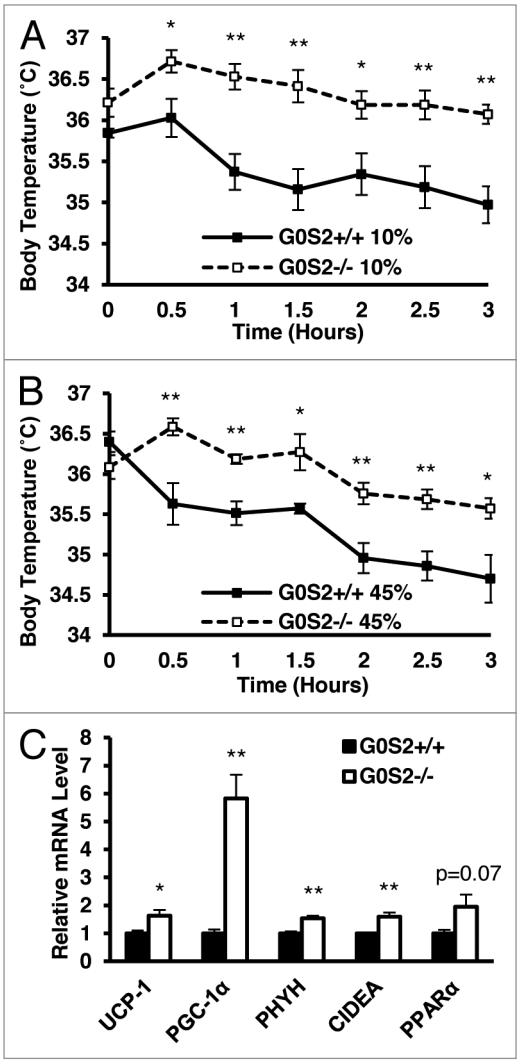

Figure 6. G0S2$^{-/-}$ mice had improved cold tolerance. (**A and B**) Body temperatures of 7-mo-old male mice fed with a 10% fat diet (**A**) and a 45% fat diet (**B**) were determined during exposure to 4 °C for 3 h ($n = 7$). (**C**) Real-time PCR analysis of gene products involved in thermogenesis and fatty acid oxidation in brown adipose tissue (BAT) of G0S2$^{+/+}$ and G0S2$^{-/-}$ mice fed with a 10% fat diet following 3 h of cold exposure (4 °C) ($n = 4$). Data are presented as mean ± SE. The symbols * and ** depict statistical significance as $P < 0.05$ and $P < 0.01$, respectively.

study provides a new engineered mouse model as a tool to study G0S2 function in vivo, and extends the understanding of G0S2 function in lipid metabolism. As G0S2 is involved in lipid metabolism, cancer and immune regulation, this model will allow us to explore whether these different functions of G0S2 are directly linked to each other, and whether they are ATGL-dependent or -independent.

Materials and Methods

Generation of G0S2$^{-/-}$ mice

G0S2$^{+/-}$ mice in the C57Bl/6 strain background were generated by the trans-National Institute of Health (NIH) Knockout Mouse Project (KOMP) and obtained from the KOMP Repository. In brief, G0S2-null VGB6 embryonic stem (ES) cells isolated from the C57Bl/6NTac mouse strain were generated by KOMP. The G0S2 coding region was replaced by a lacZ and loxP-flanked neomycin resistance gene cassette and the lacZ gene was fused in-frame at the G0S2 ATG start codon. Targeting was confirmed by PCR analyses and these cells were injected into Albino C57Bl/6 blastocysts and transferred into pseudo-pregnant recipient mice. Mice with a high degree of coat color chimerism were bred with C57Bl/6 mice to test for germ line transmission. F1 mice G0S2$^{+/-}$ were intercrossed to generate G0S2$^{+/+}$, G0S2$^{+/-}$, and G0S2$^{-/-}$ mice. The G0S2$^{-/-}$ genotype was confirmed by PCR analysis of tail tip DNA using DNeasy Blood and Tissue Kit (Qiagen, 69504) and HotStar taq DNA polymerase (Qiagen, 203203) with primers used as follow: G0S2 forward primer: 5′-CTGCGGGAAG CGTGTGAAC-3′, reverse primer: 5′-ATCACAGTGC GTGCTGCAC-3′; lacZ forward primer: 5′- GGTAAACTGG CTCGGATTAG GG-3′, reverse primer: 5′- TTGACTGTAG CGGCTGATGT TG-3′. Age- and gender-matched mice were used for the described experiments. All mice were housed in a standard pathogen-free facility on a 12 h light 12 h dark cycle and they had continuous access to water and regular food chow (Harlan Laboratories). Protocols for the animal studies were approved by Dartmouth's Institutional Animal Care and Usage Committee (IACUC).

Immunoblot analysis

To confirm knockout of G0S2 at the protein level, white adipose tissue was harvested from 3 mo old male G0S2$^{+/+}$ and G0S2$^{-/-}$ mice, respectively. Tissues were immediately snap-frozen and homogenized in radioimmunoprecipitation assay buffer to extract proteins. Immunoblot assays were performed with procedures, as previously described.[29] G0S2 protein was probed with an anti-G0S2 antibody[6] and actin was probed with an anti-actin antibody (C19) (Santa Cruz Biotechnology, sc-1615).

Tissue isolation and lacZ staining

Male G0S2$^{+/+}$, G0S2$^{+/-}$, and G0S2$^{-/-}$ mice were sacrificed at 3 mo of age, according to IACUC-approved procedures. Indicated organs were harvested and fixed in 4% paraformaldehyde (Electron Microscopy Sciences, 15713) on ice for 2 h and then cryoprotected in 30% sucrose at 4 °C (Schwarz Mann, 909530) overnight.[30] Tissues were then embedded in Tissue-Tek O.C.T. compound (Ted Pella, 27050) and cryosections were each made at a 10 μm thickness. Tissue slides were fixed with 4% paraformaldehyde for 10 min at 4 °C. Slides were then washed with phosphate buffered saline (PBS) and then rinsed with distilled water. Afterwards, slides were stained with 5-bromo-4-chloro-3-indoyl-β-D-galactoside (X-gal, Invitrogen, B1690) at 37 °C in a humidified chamber. Tissue slides were then stained with nuclear fast red solution (Sigma, N3020-100ML) for counterstaining and were mounted with Permount medium (Thermo Fisher, SP15-500).

Diet-induced obesity

Male mice at 8 wk of age were fed a 10% fat diet (control diet) or 45% fat diet (high fat diet [HFD], 39.4% lard and 5.6% soybean oil) ad libitum (Research Diets, D12450B and D12451, respectively) for 14 wk. Body weight and food intake were

monitored once a week. Relative body weight was calculated by normalizing body weight of each mouse to its initial body weight, given that each G0S2 engineered line (+/+, −/−) varied in their respective body weights at the beginning of these experiments.

Serum analysis

Serum parameters were analyzed for mice fed with 10% fat diet ad libitum. Free FA levels were measured using a free FA quantification kit (BioVision, K612-100) and glycerol levels were measured using a free glycerol assay kit (BioVision, K630-100) according to the manufacturer's protocols.

Metabolic measurements

O_2 consumption, CO_2 production, RQ, and active time were each measured at 23 °C ambient temperature for 24 h with access to food and water ad libitum with a 7 am–7 pm light on and 7 pm–7 am light off cycle in a metabolic chamber. Inner dimensions for the metabolic chamber were 10 × 10 × 8 cm and a motion sensor piezosensor[31] was embedded in gel in the base. After 2 h acclimation in the metabolic chamber, individual O_2 consumption and CO_2 production were recorded every 1 s by an O_2 analyzer S-3A/I (Applied Electrochemistry) and CO_2 analyzer CD-3A (Applied Electrochemistry), respectively. Activity was measured concurrently through the piezosensor. RQ is the O_2 consumption divided by the CO_2 production. Mean hour O_2 consumption, CO_2 production, RQ, and active time were determined for each mouse.

Cold exposure assays

Individual mice were placed in a 4 °C cold room for 3 h in the absence of food in a cage. Body temperature was independently measured at 0 (right before entering the cold room), 30, 60, 90, 120, 150, and 180 min after cold exposure using a rectal probe (Traceable Type K Thermometer, Thermo Fisher).

RNA extraction and real-time PCR assays

Brown adipose tissues were harvested right after mice were exposed to 4 °C ambient temperature for 3 h and were snap-frozen in liquid nitrogen. Total RNA was isolated from brown adipose tissue using the RNeasy Plus Universal Kit (Qiagen, 73404). Reverse transcription and real-time PCR assays were performed, as previously described.[32] Primer sequences are as follows: uncoupling protein-1 (UCP-1), forward primer: 5′-GTGAAGGTCA GAATGCAAGC-3′; reverse primer: 5′-AGGGCCCCCT TCATGAGGTC-3′; PGC1α forward primer: 5′-CAACATGCTC AAGCCAAACC AACA-3′; reverse primer: 5′-CGCTCAATAG TCTTGTTCTC AAATGGG-3′; phytanoyl-CoA dioxygenase (PHYH) forward primer: 5′-TACTGCCTTC TCCCCGAGAT-3′; reverse primer: 5′-CGGGATGTCT TCTTGCCAAC -3′; cell death-inducing DNA fragmentation factor-α-like effector A (CIDEA) forward primer: 5′-GGCCGTGTTA AGGAATCTGC-3′; reverse primer: 5′-GTATGTGCCC GCATAGACCA-3′; PPARα forward primer: 5′-TATCTCACCG GGAGGCGTT-3′; reverse primer: 5′-AGAGCGCTAA GCTGTGATGA-3′; GAPDH forward primer: 5′-AGGTCGGTGT GAACGGATTT G-3′; and reverse primer: 5′-TGTAGACCAT GTAGTTGAGG TCA-3′. Data were normalized to GAPDH levels.

Statistics

Two-tailed *t* test were used for statistical analysis with Microsoft Excel software and with $P < 0.05$ considered as statistically significant.

Note Added in Proof

While this paper was under review, Zhang et al.[33] reported on mice null for the G0S2 gene. Consistent with our data they also saw an attenuation of weight gain and adiposity in mice lacking G0S2.

Disclosure of Potential Conflicts of Interest

No potential conflicts of interest were disclosed.

Acknowledgments

This study was supported by National Institutes of Health (NIH) and National Cancer Institute (NCI) grants R01-CA087546 (E.D. and S.J.F.), R01-CA062275 (E.D.) and R01-CA111422 (E.D. and S.J.F.); by a Samuel Waxman Cancer Research Foundation award (E.D.); by an American Cancer Society Clinical Research Professorship (E.D.) provided by a generous gift from the FM Kirby Foundation; by a Prouty Multi-Investigator Award (S.J.F.), and by a grant from Uniting Against Lung Cancer with Mary Jo's Fund to Fight Cancer (S.J.F.). Dartmouth's Norris Cotton Cancer Center Shared Resources were used and supported by NCI Core Grant 5P30CA023108. We thank Dr Radu Stan (Geisel School of Medicine at Dartmouth) for photographing lacZ staining slides.

References

1. Siderovski DP, Blum S, Forsdyke RE, Forsdyke DR. A set of human putative lymphocyte G0/G1 switch genes includes genes homologous to rodent cytokine and zinc finger protein-encoding genes. DNA Cell Biol 1990; 9:579-87; PMID:1702972; http://dx.doi.org/10.1089/dna.1990.9.579
2. Yang X, Lu X, Lombès M, Rha GB, Chi Y-I, Guerin TM, Smart EJ, Liu J. The G(0)/G(1) switch gene 2 regulates adipose lipolysis through association with adipose triglyceride lipase. Cell Metab 2010; 11:194-205; PMID:20197052; http://dx.doi.org/10.1016/j.cmet.2010.02.003
3. Schweiger M, Paar M, Eder C, Brandis J, Moser E, Gorkiewicz G, Grond S, Radner FPW, Cerk I, Cornaciu I, et al. G0/G1 switch gene-2 regulates human adipocyte lipolysis by affecting activity and localization of adipose triglyceride lipase. J Lipid Res 2012; 53:2307-17; PMID:22891293; http://dx.doi.org/10.1194/jlr.M027409
4. Zandbergen F, Mandard S, Escher P, Tan NS, Patsouris D, Jatkoe T, Rojas-Caro S, Madore S, Wahli W, Tafuri S, et al. The G0/G1 switch gene 2 is a novel PPAR target gene. Biochem J 2005; 392:313-24; PMID:16086669; http://dx.doi.org/10.1042/BJ20050636
5. Yamada T, Park CS, Burns A, Nakada D, Lacorazza HD. The cytosolic protein G0S2 maintains quiescence in hematopoietic stem cells. PLoS One 2012; 7:e38280; PMID:22693613; http://dx.doi.org/10.1371/journal.pone.0038280
6. Kitareewan S, Blumen S, Sekula D, Bissonnette RP, Lamph WW, Cui Q, Gallagher R, Dmitrovsky E. G0S2 is an all-trans-retinoic acid target gene. Int J Oncol 2008; 33:397-404; PMID:18636162
7. Welch C, Santra MK, El-Assaad W, Zhu X, Huber WE, Keys RA, Teodoro JG, Green MR. Identification of a protein, G0S2, that lacks Bcl-2 homology domains and interacts with and antagonizes Bcl-2. Cancer Res 2009; 69:6782-9; PMID:19706769; http://dx.doi.org/10.1158/0008-5472.CAN-09-0128
8. Kusakabe M, Watanabe K, Emoto N, Aki N, Kage H, Nagase T, Nakajima J, Yatomi Y, Ohishi N, Takai D. Impact of DNA demethylation of the G0S2 gene on the transcription of G0S2 in squamous lung cancer cell lines with or without nuclear receptor agonists. Biochem Biophys Res Commun 2009; 390:1283-7; PMID:19878646; http://dx.doi.org/10.1016/j.bbrc.2009.10.137
9. Kusakabe M, Kutomi T, Watanabe K, Emoto N, Aki N, Kage H, Hamano E, Kitagawa H, Nagase T, Sano A, et al. Identification of G0S2 as a gene frequently methylated in squamous lung cancer by combination of in silico and experimental approaches. Int J Cancer 2010; 126:1895-902; PMID:19816938

10. Tokumaru Y, Yamashita K, Osada M, Nomoto S, Sun D-I, Xiao Y, Hoque MO, Westra WH, Califano JA, Sidransky D. Inverse correlation between cyclin A1 hypermethylation and p53 mutation in head and neck cancer identified by reversal of epigenetic silencing. Cancer Res 2004; 64:5982-7; PMID:15342377; http://dx.doi.org/10.1158/0008-5472.CAN-04-0993
11. Walther TC, Farese RV Jr. Lipid droplets and cellular lipid metabolism. Annu Rev Biochem 2012; 81:687-714; PMID:22524315; http://dx.doi.org/10.1146/annurev-biochem-061009-102430
12. Haemmerle G, Lass A, Zimmermann R, Gorkiewicz G, Meyer C, Rozman J, Heldmaier G, Maier R, Theussl C, Eder S, et al. Defective lipolysis and altered energy metabolism in mice lacking adipose triglyceride lipase. Science 2006; 312:734-7; PMID:16675698; http://dx.doi.org/10.1126/science.1123965
13. German JB. Dietary lipids from an evolutionary perspective: sources, structures and functions. Matern Child Nutr 2011; 7(Suppl 2):2-16; PMID:21366863; http://dx.doi.org/10.1111/j.1740-8709.2011.00300.x
14. Ouellet V, Labbé SM, Blondin DP, Phoenix S, Guérin B, Haman F, Turcotte EE, Richard D, Carpentier AC. Brown adipose tissue oxidative metabolism contributes to energy expenditure during acute cold exposure in humans. J Clin Invest 2012; 122:545-52; PMID:22269323; http://dx.doi.org/10.1172/JCI60433
15. Haman F. Shivering in the cold: from mechanisms of fuel selection to survival. J Appl Physiol (1985) 2006; 100:1702-8; PMID:16614367; http://dx.doi.org/10.1152/japplphysiol.01088.2005
16. Kobayashi S, Ito A, Okuzaki D, Onda H, Yabuta N, Nagamori I, Suzuki K, Hashimoto H, Nojima H. Expression profiling of PBMC-based diagnostic gene markers isolated from vasculitis patients. DNA Res 2008; 15:253-65; PMID:18562305; http://dx.doi.org/10.1093/dnares/dsn014
17. Nakamura N, Shimaoka Y, Tougan T, Onda H, Okuzaki D, Zhao H, Fujimori A, Yabuta N, Nagamori I, Tanigawa A, et al. Isolation and expression profiling of genes upregulated in bone marrow-derived mononuclear cells of rheumatoid arthritis patients. DNA Res 2006; 13:169-83; PMID:17082220; http://dx.doi.org/10.1093/dnares/dsl006
18. Koczan D, Guthke R, Thiesen H-J, Ibrahim SM, Kundt G, Krentz H, Gross G, Kunz M. Gene expression profiling of peripheral blood mononuclear leukocytes from psoriasis patients identifies new immune regulatory molecules. Eur J Dermatol 2005; 15:251-7; PMID:16048752
19. Russell TD, Schaack J, Orlicky DJ, Palmer C, Chang BH-J, Chan L, McManaman JL. Adipophilin regulates maturation of cytoplasmic lipid droplets and alveolae in differentiating mammary glands. J Cell Sci 2011; 124:3247-53; PMID:21878492; http://dx.doi.org/10.1242/jcs.082974
20. Ahmadian M, Duncan RE, Varady KA, Frasson D, Hellerstein MK, Birkenfeld AL, Samuel VT, Shulman GI, Wang Y, Kang C, et al. Adipose overexpression of desnutrin promotes fatty acid use and attenuates diet-induced obesity. Diabetes 2009; 58:855-66; PMID:19136649; http://dx.doi.org/10.2337/db08-1644
21. Zhang L-H, Zhang L-J, Wang Q, Wang B, Yang G-S. Expression of TGH and its role in porcine primary adipocyte lipolysis. Mol Cell Biochem 2008; 315:159-67; PMID:18543084; http://dx.doi.org/10.1007/s11010-008-9800-y
22. Holm C. Molecular mechanisms regulating hormone-sensitive lipase and lipolysis. Biochem Soc Trans 2003; 31:1120-4; PMID:14641008; http://dx.doi.org/10.1042/BST0311120
23. Okazaki H, Igarashi M, Nishi M, Tajima M, Sekiya M, Okazaki S, Yahagi N, Ohashi K, Tsukamoto K, Amemiya-Kudo M, et al. Identification of a novel member of the carboxylesterase family that hydrolyzes triacylglycerol: a potential role in adipocyte lipolysis. Diabetes 2006; 55:2091-7; PMID:16804080; http://dx.doi.org/10.2337/db05-0585
24. Granneman JG, Burnazi M, Zhu Z, Schwamb LA. White adipose tissue contributes to UCP1-independent thermogenesis. Am J Physiol Endocrinol Metab 2003; 285:E1230-6; PMID:12954594
25. Jensen DR, Knaub LA, Konhilas JP, Leinwand LA, MacLean PS, Eckel RH. Increased thermoregulation in cold-exposed transgenic mice overexpressing lipoprotein lipase in skeletal muscle: an avian phenotype? J Lipid Res 2008; 49:870-9; PMID:18175800; http://dx.doi.org/10.1194/jlr.M700519-JLR200
26. Shabalina IG, Hoeks J, Kramarova TV, Schrauwen P, Cannon B, Nedergaard J. Cold tolerance of UCP1-ablated mice: a skeletal muscle mitochondria switch toward lipid oxidation with marked UCP3 up-regulation not associated with increased basal, fatty acid- or ROS-induced uncoupling or enhanced GDP effects. Biochim Biophys Acta 2010; 1797:968-80; PMID:20227385; http://dx.doi.org/10.1016/j.bbabio.2010.02.033
27. Yamada T, Park CS, Shen Y, Rabin KR, Lacorazza HD. G0S2 inhibits the proliferation of K562 cells by interacting with nucleolin in the cytosol. Leuk Res 2014; 38:210-7; PMID:24183236; http://dx.doi.org/10.1016/j.leukres.2013.10.006
28. Mongelard F, Bouvet P. Nucleolin: a multiFACeTed protein. Trends Cell Biol 2007; 17:80-6; PMID:17157503; http://dx.doi.org/10.1016/j.tcb.2006.11.010
29. Ma T, Fuld AD, Rigas JR, Hagey AE, Gordon GB, Dmitrovsky E, Dragnev KH. A phase I trial and in vitro studies combining ABT-751 with carboplatin in previously treated non-small cell lung cancer patients. Chemotherapy 2012; 58:321-9; PMID:23147218; http://dx.doi.org/10.1159/000343165
30. Náray-Fejes-Tóth A, Fejes-Tóth G. Novel mouse strain with Cre recombinase in 11beta-hydroxysteroid dehydrogenase-2-expressing cells. Am J Physiol Renal Physiol 2007; 292:F486-94; PMID:16896181; http://dx.doi.org/10.1152/ajprenal.00188.2006
31. Megens AA, Voeten J, Rombouts J, Meert TF, Niemegeers CJ. Behavioral activity of rats measured by a new method based on the piezo-electric principle. Psychopharmacology (Berl) 1987; 93:382-8; PMID:3124168; http://dx.doi.org/10.1007/BF00187261
32. Ma T, Dong JP, Sekula DJ, Fei DL, Lamph WW, Henderson M, Lu Y, Blumen S, Freemantle SJ, Dmitrovsky E. Repression of exogenous gene expression by the retinoic acid target gene G0S2. Int J Oncol 2013; 42:1743-53; PMID:23546556
33. Zhang X, Xie X, Heckmann BL, Saarinen AM, Czyzyk TA, Liu J. Targeted disruption of g0/g1 switch gene 2 enhances adipose lipolysis, alters hepatic energy balance, and alleviates high-fat diet-induced liver steatosis. Diabetes 2014; 63:934-46; PMID:24194501; http://dx.doi.org/10.2337/db13-1422